

Inverse Filters for Decomposition of Multi-Exponential and Related Signals

VAIRIS SHTRAUSS
 Institute of Polymer Mechanics
 University of Latvia
 23 Aizkraukles Street, LV 1006 Riga
 LATVIA

Abstract: - Decomposition of multi-exponential and related signals is generalized as a filtering problem on a logarithmic time or frequency scale and FIR filters operating with logarithmically sampled data are proposed to use for its implementation. The filter algorithms and types are found for various time-domain and frequency-domain mono-components. It is demonstrated that the ill-posedness in the multi-component decomposition manifests as high sampling-rate dependent noise amplification coefficients. The noise transformation control of a filter is provided by algorithm design, which integrates together the signal acquisition, the discrete-time filter design and the regularization based on choosing an optimum sampling rate. As an example, an algorithm is designed for the decomposition in the frequency-domain.

Key-Words: - Decomposition, Distribution of Time Constants, FIR Filters, Logarithmic Sampling, Ill-posedness, Regularization

1 Introduction

Many areas of science and technology, such as material science, mechanics, biology, nuclear and electrical engineering, etc. face the problem of analysing monotonic and locally monotonic signals. The multi-component signals with the real decaying exponentials are probably the most studied case, although the similar problems arise for many other monotonic mono-components, such as integrals, derivatives, real and imaginary parts of the Fourier transforms of the real exponentials.

Although the analysis of monotonic signals is not new, let remember the classical Gardner work [1] published almost 50 years ago, and is widely studied in various fields [2-6], and especially in relaxation spectroscopy [7-9], the problem remains a challenging signal processing task. The principal reasons are the exceedingly non-orthogonal behaviour of the monotonic signals no constituting an orthogonal base, and the fundamental ill-posedness in the sense that small perturbations in input signal can yield unrealistic high perturbations in the decomposition results.

Motivation of this work is to find new possibilities for analysing multi-component monotonic signals based on the up-to-date data processing technologies [10] and to derive accurate, robust and computationally efficient algorithms.

2 Monotonic Multi-component Signals

Multi-exponential decays may be described by the following model

$$x(t) = \int_0^{\infty} G(\tau) \exp(-t/\tau) d\tau, \tag{1}$$

where $G(\tau)$ is a function of *distribution of time constants* (DTC) or *spectrum of time constants*. For the discrete (line) spectrum, $G(\tau)$ takes the form

$$G(\tau) = \sum_n G_n \delta(\tau - \tau_n),$$

where $\delta(\tau)$ is the Dirac delta function.

In some fields, e.g. in relaxation studies [7-9], Eq. (1) is modified in the form

$$x(t) = \int_0^{\infty} F(\tau) \exp(-t/\tau) d\tau / \tau, \tag{2}$$

where the new, so-called logarithmic DTC function $F(\tau) = G(\tau)\tau$, is introduced.

To generalize model (2) for other monotonic and locally monotonic signals, we modify it into the form

$$x(u) = \int_0^{\infty} F(\tau) K(u, \tau) d\tau / \tau, \tag{3}$$

where variable u is time or frequency, and kernel $K(u, \tau)$ represents a family of the time-domain and frequency-domain mono-components being of great importance in various fields

$$K(u, \tau) = \begin{cases} \exp(-u/\tau) & (4a) \\ \exp(-u/\tau)/\tau & (4b) \\ 1 - \exp(-u/\tau) & (4c) \\ 1/(1+u^2\tau^2) & (4d) \\ u\tau/(1+u^2\tau^2) & (4e) \\ u^2\tau^2/(1+u^2\tau^2) & (4f) \end{cases}$$

Kernels (4b) and (4c) represent the derivative and integral, respectively, of the basic real decaying exponential (4a). In its turn, kernels (4d) and (4e) embodies the real parts and imaginary parts of the Fourier transform of (4b). A pair of kernels (4f) and (4e) describes the frequency response of the system inverse to that characterized by a pair of kernels (4d) and (4e).

3 Filtering Approach for DTC Recovery

3.1 Background

Since kernels (4a) – (4f) depend on the ratio or product of arguments u and τ , model (3) may be converted in the form of the Mellin convolution type transform

$$x(u) = F \overset{M}{*} k = \int_0^\infty F(\tau)k(u/\tau)d\tau/\tau \quad (5)$$

where $\overset{M}{*}$ denotes the Mellin convolution and $k(u)$ are kernels (4a) – (4f) modified in the form needed for converting Eq. (3) into Eq. (5) (canonic kernels [11]).

Monotonic multi-component signals (3) are typically recorded over long intervals of time or broad ranges of frequency [7-9], due to this, it is useful to consider them on a logarithmic scale

$$u^* = \log_q u/u_0, \quad (6)$$

where u_0 is an arbitrary normalization constant. For logarithmic arguments (6), to remember that $u = u_0 q^{u^*}$, Eq. (5) alters into the appropriate Fourier convolution type transform ($u_0 = 1$)

$$x(q^{u^*}) = F(q^{u^*}) \overset{F}{*} k(q^{u^*}).$$

Consequently, DTC may be formally determined by the appropriate deconvolution

$$F(q^{u^*}) = x(q^{u^*}) \overset{F}{*} k^{-1}(q^{u^*}), \quad (7)$$

which can be considered as an ideal DTC estimator. Deconvolution (7) represents a *linear shift-invariant system* or an *ideal filter* [10] on a logarithmic time or frequency domain with impulse responses $k^{-1}(q^{u^*})$ existing in the sense of generalized functions. The analytic expressions of $k^{-1}(q^{u^*})$ are not known, however one may derive the appropriate frequency responses as the reciprocals of the Mellin transforms of canonic kernels $k(u)$

$$H(j\mu) = 1/M[k(u); -j\mu] = 1/\int_0^\infty k(u)u^{-j\mu-1}du, \quad (8)$$

where parameter μ named the Mellin frequency [12] represents the frequency of a signal (function), whose independent variable (time or frequency) is logarithmically transformed.

In the frequency domain, deconvolution (7) may be described as

$$F_T(j\mu) = X(j\mu)/K(j\mu) \quad (9)$$

where $F_T(j\mu)$, $X(j\mu)$ and $K(j\mu)$ are the Fourier transforms of functions $F(q^{u^*})$, $x(q^{u^*})$ and $k(q^{u^*})$ with logarithmically transformed arguments. At the same time, $F_T(j\mu)$, $X(j\mu)$ and $K(j\mu)$ represent also the Mellin transforms of original functions $F(u)$, $x(u)$ and $k(u)$ on linear scale.

Spectral representation (9) is a basis of the classical methods of Gardner [1], Schlesinger [2] and Roesler [3] implementing the decomposition by the following general scheme

$$F[\tau_m] = \text{IDFT}\{\text{DFT}[x(q^{u^*})]/\text{DFT}[k(q^{u^*})]\}, \quad (10)$$

where IDFT and DFT are abbreviations of direct and inverse discrete Fourier transforms. Similarly, spectral representation (9) is used in the method Prost and Goutte [4,5] implementing the decomposition by the direct and inverse discrete Mellin transforms ((DMT) and (IDMT))

$$F[\tau_m] = \text{IDMT}\{\text{DMT}[x(u)]/\text{DMT}[k(u)]\}. \quad (11)$$

Our idea is to implement deconvolution (7) in direct way by a FIR filter operating with equally

spaced samples on a logarithmic scale, which may be represented in the following non-causal algorithm

$$F(u_m^*) = \sum_{n=-\infty}^{\infty} h[n]x(u_{m-n}^*), \quad (12)$$

where $h[n]$ is impulse response, which, of course, must be limited to the finite length in practice.

To take into consideration that equally spaced samples on a logarithmic scale manifest as the logarithmically sampled data on linear scale where distance between samples increases according to the geometric progression

$$u_m^* = u_0 q^m, \quad m = 0, \pm 1, \pm 2, \dots,$$

algorithm (12) modifies into the following general form:

$$F(u_0 q^m) = \sum_{n=-\infty}^{\infty} h[n]x(u_0 q^{m-n}). \quad (13a)$$

Direct implementation of the deconvolution by FIR filter has some advantages. First, its realization with hardware or software is much simpler. Second, the direct implementation can potentially give the higher accuracy because does not require to perform the Mellin or Fourier transform of the noisy signals to be limited by a finite length window contributing the basic errors in approaches (10) and (11).

3.2 Algorithms of DTC estimators

Eq. (3) with kernels (4a) and (4c) forms exactly the Mellin convolution type transform (5), for which algorithm (13a) can be directly applied to. For the other kernels of Eq. (4), general algorithm (13a) modifies into the following two sub-algorithms

$$F(u_0 q^m) = \begin{cases} u_0 q^m \sum_{n=-\infty}^{\infty} h[n]x(u_0 q^{m-n}) & (13b) \\ \sum_{n=-\infty}^{\infty} h[n]x(q^{-m-n} / u_0) & (13c) \end{cases}$$

where Eq. (13b) relates to kernel (4b), while Eq. (13c) relates to the frequency-domain data, i.e. to kernels (4d) – (4f).

Usually [11,12], the considered here filters are used with the equal number of coefficients about their origins. Thus, for odd number of filter coefficients N , general algorithm (13a) takes the form

$$F(u_0 q^m) = \sum_{n=-(N-1)/2}^{(N-1)/2} h[n]x(u_0 q^{m-n}),$$

where the origin of impulse response coincides with zero sample $h[0]$. For even number of filter coefficients, the origin of impulse response may be located in the middle between the samples $h[-1]$ and $h[0]$, then algorithm (13a) modifies into the form

$$F(u_0 q^m) = \sum_{n=-(N-2)/2-1}^{(N-2)/2} h[n]x(u_0 q^{m-0.5-n}).$$

3.3 Types of DTC estimators

For six kernels (4a) – (4f), Eq. (8) gives the **three** following ideal frequency responses

$$H(j\mu) = \begin{cases} -1/\Gamma(-j\mu) & \text{for (4a) – (4c)} & (14a) \\ \pm j2\text{sh}(\pi\mu)/\pi & \text{for (4d) and (4f)} & (14b) \\ 2\text{ch}(\pi\mu)/\pi & \text{for (4e)} & (14c) \end{cases}$$

i.e. for the time-domain data, for the real parts, and for the imaginary parts, respectively. Consequently, only **three independent** sets of coefficients $h[n]$ are necessary for implementing decomposition (3) for six kernels (4a) – (4f). The filters have similar – very steep growing magnitude responses (Fig. 1) indicating their inverse nature [11].

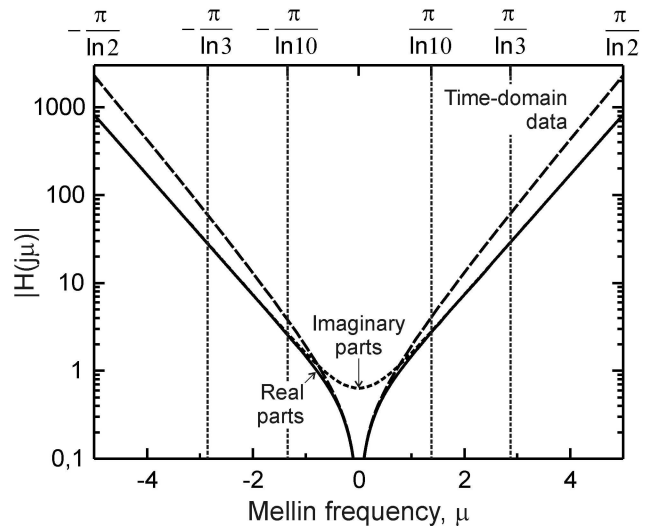


Fig. 1. Magnitude responses of the three ideal DTC estimators. Vertical lines and upper X-axis show the bandwidths corresponding to different q .

Frequency response (14a) of the ideal DTC estimator employing the time-domain data is a complex function. From the symmetry property of

the Fourier transform [10], it follows that the appropriate impulse response has no symmetry, or, in other words, the estimators recovering DTC from the time-domain data belong to so-called *non-linear phase systems*.

In contrast, frequency response (14b) is a pure imaginary function, while response (14c) is a real function. This indicates that the estimators recovering DTC from the frequency-domain data are *linear phase systems* [10].

In Fig. 2(a, c), schematic approximation of ideal frequency response (14b) is shown by the appropriate frequency responses of a discrete-time filter

$$H(e^{j\mu}) = \sum_n h[n] \exp(-j\mu n \ln q) \quad (15)$$

with odd and even number of coefficients.

In the case of odd number of coefficients, the estimator represents *type III linear phase filter* [10] having the frequency response, which crosses zero at the ends of bandwidth $\mu = \pm\pi / \ln q$ and at zero frequency (Fig. 2(a)). It has the anti-symmetric impulse response ($h[n] = -h[-n]$) (Fig. 2(c)). In the case of even number of coefficients, the estimator represents *type IV linear phase filter* having the frequency response crossing zero at zero frequency and having non-zero values at the ends of the bandwidth $\mu = \pm\pi / \ln q$ (Fig. 2(b)). It has an anti-symmetric impulse response ($h[n] = -h[-n - 1]$) (Fig. 2(d)).

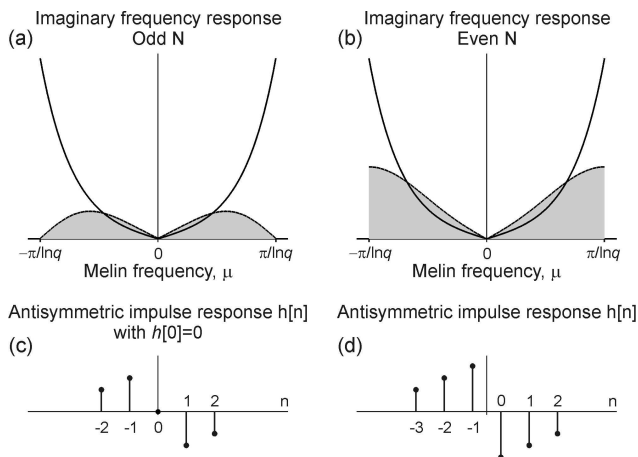


Fig. 2. Schematic approximation of frequency response (14b) with odd (a) and even (b) number of coefficients, and examples of the appropriate discrete impulse responses (c) and (d).

In Fig. 3, the similar plots are shown for an estimator with ideal frequency response (14c)

employing the imaginary parts. In this case, the estimator with odd number of coefficients represents *type I linear phase filter* having the symmetric impulse response ($h[n] = h[-n]$) (Fig. 3(c)), while the estimator with even number of coefficients represents *type II linear phase filter* having the symmetric impulse response ($h[n] = -h[-n - 1]$) (Fig. 3(d)).

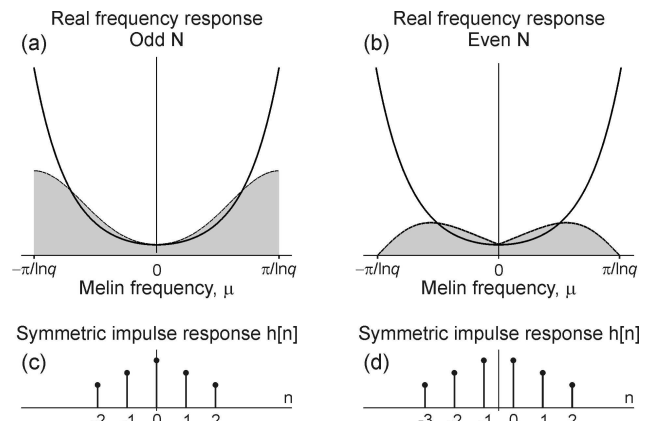


Fig. 3. Schematic approximation of frequency response (14c) with odd (a) and even (b) number of coefficients, and examples of the appropriate discrete impulse responses (c) and (d).

4 Noise Behaviour and Ill-posedness

The decomposition is characteristically ill-posed in the sense that small perturbations in multi-component signal can yield unrealistic high perturbations in the output DTC. The noise behaviour of a DTC estimator is characterized by *noise coefficient S* transforming input noise (random error) variance σ_x^2 into the output noise variance σ_y^2

$$\sigma_y^2 = S\sigma_x^2$$

being equal to sum of the square filter coefficients

$$S_\sigma = \sum_{n=1}^N h^2[n]. \quad (16)$$

The Parseval theorem [10] allows determining noise coefficient *S* also through frequency response

$$S = \ln q / (2\pi) \int_{-\pi/\ln q}^{\pi/\ln q} |H(\cdot)|^2 d\mu, \quad (17)$$

where ideal frequency responses (14a) – (14c) give inherent to the decomposition theoretical noise coefficients S_{theor} for the given progression ratio *q*,

while frequency responses (15) of digital estimators provides actual experimental noise coefficient (16).

As follows from Eq. (17), increasing the sampling rate (decreasing q) extends operating bandwidth $[-\pi/\ln q, \pi/\ln q]$ of a filter (see Fig. 1), and, consequently, the appropriate area under the magnitude response quoting the value of noise coefficient S . Due to the increasing frequency responses, the theoretical noise coefficient increases with decreasing progression ratio q and tends to ∞ , when q approaches 1 (see curve S_{theor} in Fig. 4). Thus, the ill-posedness of the decomposition manifests as the large noise coefficient coming the large area under magnitude response, which, in its turn, results from the wide bandwidth. It can be concluded that the ill-posedness may be controlled by progression ratio q and quantitatively characterized by the noise coefficient S .

5 Algorithm Design

Practice shows that best results for the multi-component decomposition give discrete-time filters designed by the identification method [11] where a pair of theoretical functions interrelated with each other by theoretical deconvolution (7) are used as input and output signals in the filter design. To use the identification method, the filter specification (number of filter coefficients N and progression ratio q) shall be known. According to Section 4, progression ratio q must be chosen to ensure the needed noise coefficient S . On the other hand, choice of q and N is limited by time or frequency range of available input data.

Thus, the conventional two-step signal processing approach [10] consisting of separate (i) signal acquisition step, where the signal is sampled uniformly in time above its Nyquist rate, and (ii) discrete-time algorithm implementation step, is not applicable to the decomposition, and the algorithm design must integrate together [13]: (i) signal acquisition, (ii) filter design and (iii) regularization.

The appropriate algorithm design method is described in [13]. To link q and N with input data, a parameter – the dynamic range of time or frequency of input signal portion used for computing an output sample (further ‘input window range’)

$$d_x = u_+ / u_- = q^{N-1}, \tag{18}$$

is introduced, which determines the combinations of q and N allowable for filter design.

6 Example of DTC estimator design

The below, an example of the algorithm design is considered for the frequency-domain decomposition of a multi-component signal with mono-components in the form of real parts (4d).

Let us assume that: (i) a FIR DTC estimator with even number of coefficients has to be designed; (ii) the noise coefficient S shall not exceed 10; input window range d_x shall not exceed 500.

In Fig.4, noise coefficients S are shown versus progression ratio q for various input window ranges d_x .

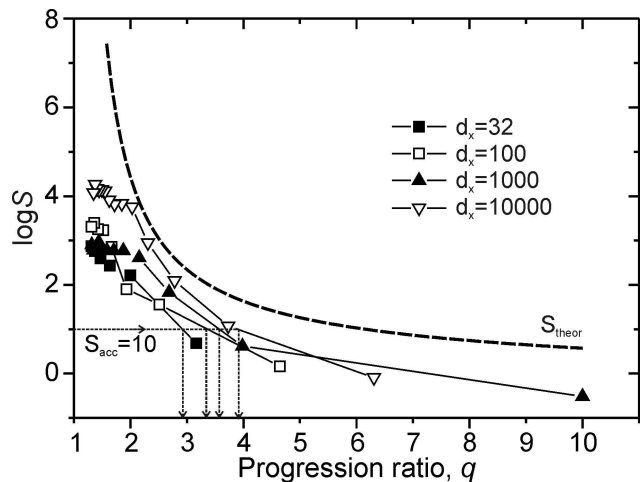


Fig. 4. Theoretical and experimental noise coefficients of DTC estimators having even number of coefficients for various input window ranges d_x . Horizontal and vertical arrows show the values of S and q corresponding to acceptable noise coefficient $S_{\text{acc}} = 10$.

From Fig. 4, it follows that to ensure noise coefficient $S_{\text{acc}} \leq 10$, progression ratio must be within interval $q = 2.9 \dots 3.9$. We choose $q = 3.3$. From Eq. (18) and condition $d_x \leq 500$, it follows that the estimator must have $N = 6$ coefficients ($d_x = 391$). By the identification method, the following coefficients have been obtained [14]:

$$h[6] = \{-0.033296, 0.129207, -1.05880, 1.05880, -0.129207, 0.033296\}$$

For noiseless data corresponding to the discrete spectrum, the designed estimator gives DTCs without non-physical oscillations (Fig. 5). It has noise coefficient $S = 2.28$, which means that the noise variance for recovered DTC is amplified 2.28 times to compare with that of the input signal or the standard deviation of DTC noise is amplified

$\sqrt{2.28} = 1.51$ times to compare with the input noise. It must be noted, that such relatively high noise immunity for an inverse filter is achieved at the expense of decreased resolution; the estimator allows separating two spectral lines only, if $\tau_{i+1} / \tau_i \leq 5.2$. In general, the proposed filtering approach is more preferable for recovering continuous DTC [14].

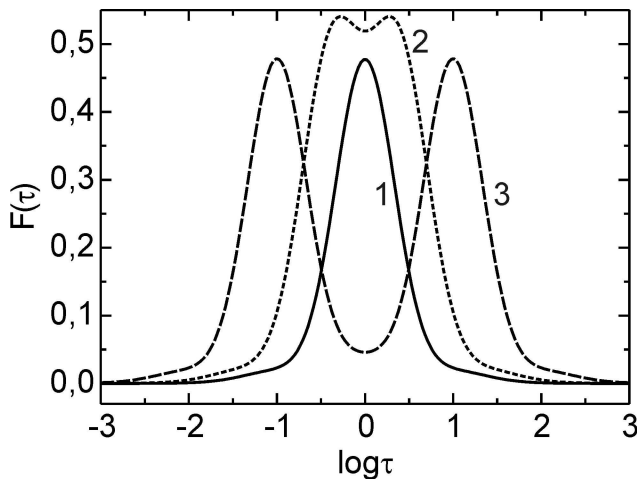


Fig. 5. Recovered DTCs for the line spectra: unity spectrum at $\tau = 1$ (curve 1); two unity line spectra at $\tau_1 = 0.42$ and $\tau_2 = 2.37$ (curve 2) and at $\tau_1 = 0.1$ and $\tau_2 = 10$ (curve 3). The recovered DTCs are calculated by algorithm (13c) modified into the form

$$F(\tau) = \sum_{n=-3}^2 h[n]x(3.3^{-0.5-n} / \tau).$$

7 Conclusions

FIR filters operating with equally sampled data on a logarithmic time or frequency scale are proposed to use for decomposition of multi-exponential and related signals, such as integrals, derivatives, real and imaginary parts of the Fourier transforms of the real exponentials. The filter algorithms are found for various time-domain and frequency-domain mono-components. It is disclosed that the non-linear phase filters are required for implementing decomposition in the time-domain, while the linear phase filters shall be used for the decomposition in the frequency-domain.

It is demonstrated that the ill-posedness in the multi-component decomposition manifests as high sampling-rate dependent noise amplification coefficients. The noise transformation control of a filter is provided by algorithm design, which integrates together the signal acquisition, the discrete-time filter design and the regularization based on choosing an optimum sampling rate.

As an example, an algorithm is designed for the decomposition in the frequency-domain.

References:

- [1] D.G. Gardner J.C. Gardner, G. Laush and W.W. Meinke, Method for analysis of multicomponent exponential decay curves, *J. Chem. Phys.*, Vol. 31, No. 4, 1959, pp. 978-986.
- [2] T. Schlesinger, Fit to experimental data with exponential functions using the fast Fourier transform, *Nucl. Instr. Meth.*, Vol. 106, No. 3, 1973, pp. 503-508.
- [3] F.C. Roesler and J.R.A. Pearson, Determination of relaxation spectra from damping measurements, *Proc. Phys. Soc.*, Vol. 67, pt. 4, No. 412B, pp. 338-347.
- [4] F.C. Roesler, Some applications of Fourier series in the numerical treatment of linear behaviour, *Proc. Phys. Soc.*, Vol. 68, pt. 2, No. 422B, pp. 89-96.
- [5] R. Prost and R. Goutte, Linear systems identification by Mellin deconvolution, *Int. J. Control*, Vol. 23, No. 4, 1976, pp. 713-720.
- [6] R. Prost and R. Goutte, Performance of the method of linear systems identifications by Mellin deconvolution, *Int. J. Control*, Vol. 25, No. 1, 1977, pp. 39-51.
- [7] J.D. Ferry, *Viscoelastic Properties of Polymers*, 3rd. ed., J. Wiley and Sons, 1980.
- [8] N.G. McCrum, B.E. Read, G. Wiliams, *Anelastic and Dielectric Effects in Polymer Solids*, J. Wiley and Sons, 1967.
- [9] A.K. Jonscher, *Dielectric Relaxation in Solids*, Chelsea Dielectric, 1983.
- [10] A. V. Oppenheim, R. V. Schafer, *Discrete-Time Signal Processing*, Sec. Ed., Prentice-Hall International, 1999.
- [11] V. Shtrauss, Functional conversion of signals in the study of relaxation phenomena, *Signal Processing*, Vol. 45, 1995, pp. 293-312.
- [12] V. Shtrauss, Digital signal processing for relaxation data conversion, *J. Non-Crystal. Solids*, Vol. 351, 2005, pp. 2911-2916.
- [13] V. Shtrauss, Sampling and algorithm design for relaxation data conversion, *WSEAS Transactions on Signal Processing*, Vol. 2, Issue 7, 2006, pp. 984-990.
- [14] V. Shtrauss, Digital Estimators of Relaxation Spectra, *J. Non-Crystal. Solids*, in press, 2007.